Available online at www.sciencedirect.com

SciVerse ScienceDirect

Physics Procedia 37 (2012) 740 – 747

Physics Procedia

TIPP 2011 – Technology and Instrumentation in Particle Physics 2011

Secondary electron yield of emissive materials for large-area micro-channel plate detectors: surface composition and film thickness dependencies

Slade J. Jokela[*a], Igor V. Veryovkin[a], Alexander V. Zinovev[a], Jeffrey W. Elam[b], Anil U. Mane[b], Qing Peng[b], Z. Insepov[c], and the Large Area Picosecond Photodetector Collaboration[d]

[a]*Argonne National Laboratory, Materials Science Division, 9700 S Cass Ave., Argonne, IL 60439, USA*
[b]*Argonne National Laboratory, Energy Systems Division, 9700 S. Cass Ave., Argonne, IL 60439, USA*
[c]*Argonne National Laboratory, Mathematics and Computing Science Division, 9700 S. Cass Ave., Argonne, IL 60439, USA*
[d]*http://psec.uchicago.edu/index.php*

Abstract

The ongoing development of Atomic Layer Deposition (ALD) enables the use of relatively inexpensive and robust borosilicate micro-channel substrates for use as Micro-Channel Plates (MCPs). The surfaces of the channels in these glass plates are functionalized to control the conductivity as well as the Secondary Electron Yield (SEY). The extensive SEY data found in literature show significant variation for a given material depending on the apparatus, the measurement procedure, and the sample preparation and handling. We present systematic studies on the effects of film thickness and surface chemical composition on SEY. We have modified an existing ultra-high vacuum apparatus containing X-ray and Ultraviolet Photoelectron Spectrometers (XPS and UPS, respectively) by adding a modified Low Energy Electron Diffraction (LEED) module for SEY measurements. With these tools, we have characterized the secondary electron emissive properties for MgO, Al_2O_3, and multilayered MgO/TiO_2 structures to serve as electron emissive layers in the channels of the MCPs.

Keywords: Secondary Electron Yield; Atomic Layer Deposition; Magnesium Oxide; Aluminum Oxide; XPS

1. Introduction

E-mail address: sjokela@anl.gov

1875-3892 doi:10.1016/j.phpro.2012.03.718

The Large-Area Picosecond Photo-Detector (LAPPD) project [1] is a collaborative effort including several national labs, universities, and companies. The group was formed with an interest in developing affordable large-area photo-detection systems. The project takes a bottom-up approach to redesigning the micro-channel plate (MCP) using technologies that have emerged after the development of the original lead-glass MCPs. The use of a non-lead glass in the MCP could substantially decreased production costs. However, the glass used in these MCPs is not suitable for electron amplification. Therefore, the MCP surface must be functionalized with conformal layers of materials having well-controlled conductivity as well as high Secondary Electron Yield (SEY). This is done using Atomic Layer Deposition (ALD), a thin film coating method that relies on alternating, self-saturating reactions between precursor vapors and a solid surface to deposit material in an atomic layer-by-layer fashion [2].

Our goal is to characterize materials useful for electron amplification in MCPs. This includes determining optimal parameters for the deposition of well known secondary electron emissive materials, such as Al_2O_3 and MgO, as well as the development of material combinations that produce enhanced SEYs.

Secondary electron emission has been studied on a broad range of materials. The data from these experiments have been gathered in databases [3] and reviewed extensively. However, different studies on the same material rarely produce results that agree. It has been known for quite some time that differences in experimental instrumentation and conditions, as well as surface composition [4, 5, 6] and morphology [7, 8] all play a role in a material's emission of secondary electrons. Thus, we feel that to better serve the LAPPD project it is necessary to conduct our own SEY measurements on the actual emissive coating materials prepared for large-area MCPs. Performing these SEY measurements together with surface composition measurements will help advance the fundamental understanding of these materials' properties.

2. Experimental Setup

To understand the influence of surface composition on the SEY, we modified a home-built X-ray photoelectron spectrometer (XPS). This system (Fig. 1) includes a hemispherical electron energy analyzer, capable of 0.9 eV energy resolution and a non-monochromated Mg Kα (1253 eV) X-ray source. To this system, we added a 5 keV Ar^+ source for sputter cleaning and milling, as well as a low energy electron diffraction (LEED) module from Vacuum Generators that was modified to measure SEY. Additionally, an electrically isolated sample holder was included in the system. This system operates under ultra-high vacuum conditions maintained by a combination of cryo-, ion-, and turbomolecular-pumps.

The LEED module includes an electron gun capable of producing a beam of electrons with kinetic energy adjustable from 5 to 1000 eV and a diameter of 500 μm. This system was modified so that the electron beam current and energy are precisely controlled by computer, allowing us to determine SEY as a function of primary electron energy. Typical electron beam currents were set in the range from 5 to 100 nA. The current was controlled by placing an appropriate bias on the emission grid, located immediately in front of the emission filament, of the electron gun. At constant current, this bias is a function of electron energy. This dependence was determined empirically by sampling the beam current over the entire parameter space (energy and emission grid bias) of the electron gun. This method allows the beam current to be rapidly set to within 50% of the intended current. Once the beam energy and current are set, the beam current varied by approximately 2% over the duration of a typical data point measurement (SEY at a fixed beam energy sampled over ~300ms). The large variation that occurs with a change in beam energy was eliminated in the SEY calculation by measuring the beam current for each data point.

Secondary electrons were collected using the LEED grids and phosphor screen, interconnected and biased at +35 V.

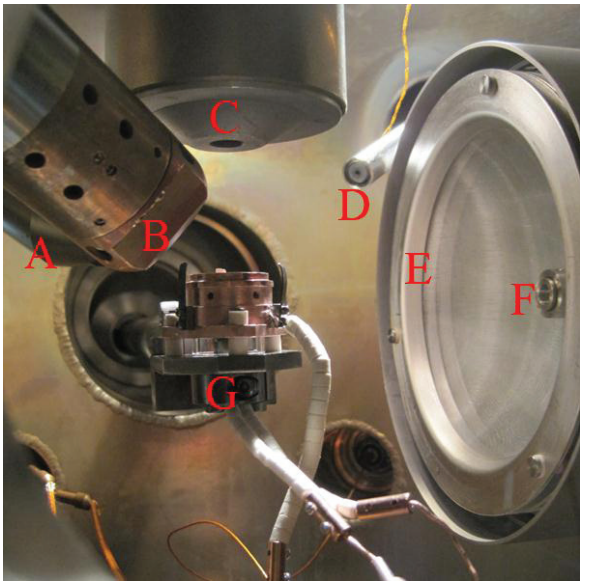

Figure 1. Photograph showing the inside of the characterization apparatus's vacuum chamber. (A) 5 keV Ar+ gun (partially obscured). (B) Mg Kα X-Ray source. (C) Hemispherical electron energy analyzer. (D) He-I UV source. (E) LEED module (grids and screens used to collect secondary electrons). (F) 5 to 1000 eV LEED electron gun (used as primary electron source). (G) Electrically isolated sample stage.

The sample holder in this system is electrically isolated, allowing us to apply a high bias voltage and to measure the net current flow through the sample. The sample holder was typically biased to -200 V to assist in secondary emission, effectively decreasing the kinetic energy range of the electron gun from 0 to 800 eV. This bias voltage was chosen based on observations showing significant increases in secondary emission as the bias was changed from 0 to -150 V, stabilizing for more negative bias voltages.

The secondary electron yield, γ, is calculated as

$$\gamma = I_{collector} / I_{beam}, \quad (1)$$

where $I_{collector}$ is the emission current collected on the LEED grids and screen, and I_{beam} is the incident primary electron beam current as measured by positively biasing the sample to suppress secondary emission. We note that this method for measurement beam current does not account for backscattered electrons, which still contribute to secondary emission. This will result in an overestimate in the SEY calculation. In the case of MgO and Al_2O_3 the percent of primary electrons lost to backscatter were estimated from Monte Carlo simulation to be 15% and 20%, respectively [9].

Also included in this system is a helium UV source capable of both He-I and He-II emission (21.2 and 40.8 eV, respectively). This source is useful for ultraviolet photoelectron spectroscopy (UPS) when used in conjunction with the hemispherical energy analyzer. However, UPS was not used in the analysis presented here.

3. Sample Preparation

Our studies included samples of Al_2O_3, MgO, MgO-TiO_2 layered structures, and TiO_2. These samples were deposited on boron-doped conductive-silicon substrates that served as "witness coupons" for MCP depositions. ALD is ideally suited for the task of placing a conformal layer of emissive materials into the channels of a MCP [1, 2]. For the studies involving SEY versus film thickness, samples of Al_2O_3 and MgO were created with controlled thicknesses ranging from 20 to 210 Å. Layered structures of MgO/TiO_2 were also created, one sample consisting of alternating 9 monolayers of MgO and 1 monolayer of TiO_2 (MgO w/ 10% TiO_2) as well as a sample of MgO with a single monolayer of TiO_2 on the surface. These samples were prepared to a thickness of 200 Å. Additionally, a sample of pure TiO_2 was prepared to a thickness of 85 Å. All "witness coupon" samples typically had lateral dimensions between 1 cm × 1 cm and 2 cm × 2 cm.

4. Experiment and Results

4.1. Secondary electron yield vs. film thickness

This study was performed to determine an optimal film thickness for the secondary emissive coating on an MCP. In this case, only Al_2O_3 and MgO were examined. While the channel of an MCP is tilted at approximately 8 degrees from the surface normal, this experiment could only be performed in our apparatus with the beam incident perpendicular to the surface. This study remains relevant since it is expected that in both cases the primary electron beam penetrates much deeper than the maximum escape depth of a secondary electron. This experiment will set an upper limit to the necessary thickness of the secondary emissive coating required to achieve maximum SEY in both cases.

Figures 2 and 3 summarize the results of these experiments. From these data, one can see that MgO is a better secondary electron emitter than Al_2O_3. For Al_2O_3, the maximum emission of 2.9 is achieved at a film thickness of 50 Å. The maximum SEY becomes saturated, remaining constant, for thicker samples. For the MgO films, in contrast, the maximum SEY continues to increase with film thickness over the entire range of films, achieving a value of 6.9 for the 200 Å film. Thicker MgO samples could not be

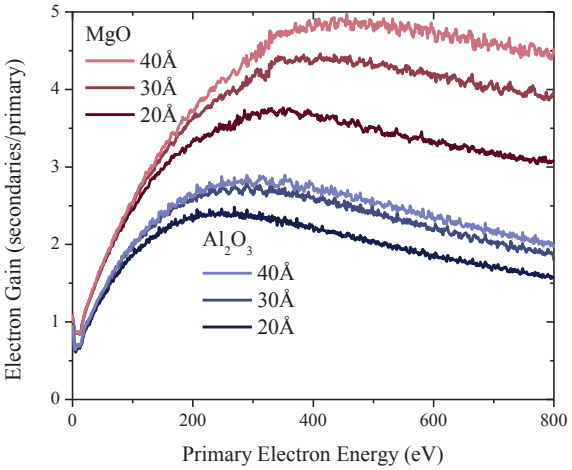

Figure 2. Secondary electron yield from select thicknesses of ALD MgO and Al_2O_3. See Figure 3 for the entire data set.

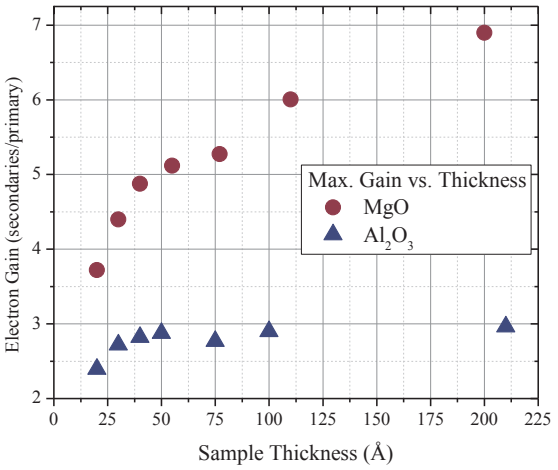

Figure 3. Maximum secondary electron yield vs. film thickness for ALD MgO and Al_2O_3. In Al_2O_3, the maximum emission is reached with a film thickness of approximately 5nm. This corresponds to the maximum escape length for a secondary electron in this sample. Sample charging limited our ability to examine thicker samples of MgO.

examined due to sample charging. This charging occurs in thicker samples because of the increased distance electrons must travel from the conductive substrate to the origin of the secondary electron [10, 11], resulting in a decreased SEY (not shown).

4.2. Secondary electron yield vs. surface composition

All samples in this work appeared to contain some amount of carbon on their surface. This is most likely due to adsorbed atmospheric carbon [12] but may also result from remnants of the organic ALD precursor molecules that may diffuse to the surface under electron bombardment [13]. The SEY of ALD

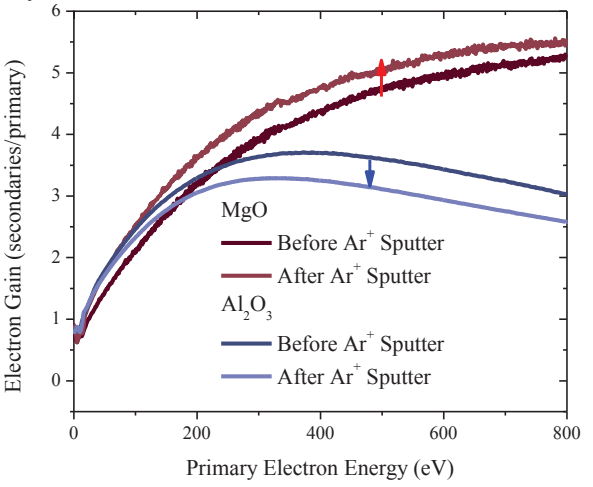

Figure 4. Comparison of 200 Å thick ALD MgO and Al_2O_3 before and after 5 keV Ar^+ sputtering. After sputtering, Al_2O_3 exhibits decreased SEY while MgO shows increased SEY. The difference in emission could be explained by differences in XPS spectra shown in Figure 5 and Figure 6. Arrows point from the as-received samples to the corresponding sample after Ar^+

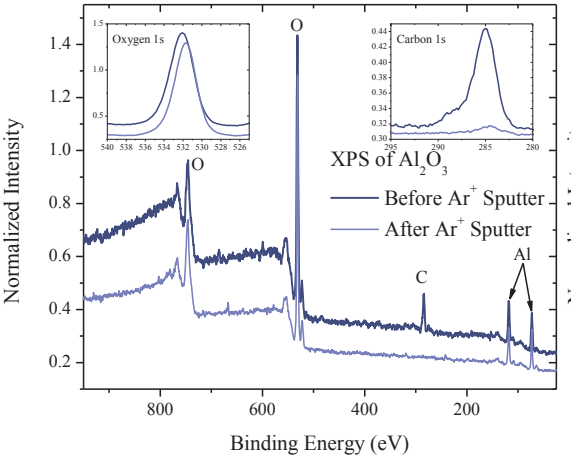

Figure 5. XPS spectra of ALD Al_2O_3. Spectra have been normalized relative to the O 1s peak height.

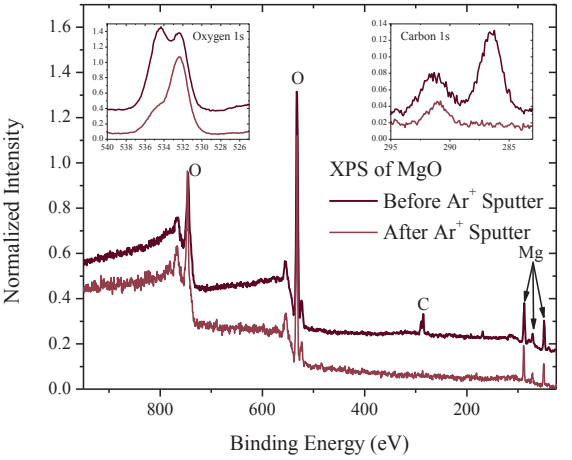

Figure 6. XPS spectrum of ALD MgO. The behavior of the double oxygen and carbon peaks (both decreasing after 5 keV Ar^+ sputtering) seems to indicate the presence of a carbon-oxygen bond that is not present in the sample of Al_2O_3 (Fig. 5). This could explain the difference in secondary electron yield behavior before and after sputtering (Fig. 4). Spectra have been normalized to O 1s peak height.

Al_2O_3 and MgO samples were measured before and after Ar^+ sputter removal of surface carbon (Fig. 4). Before sputtering, Al_2O_3 samples showed a single C 1s and a single O 1s photoelectron peak (Fig. 5). However, on MgO (Fig. 6) two C 1s and two O 1s photoelectron peaks were clearly visible, indicating the presence of two carbon species, one of which likely contains oxygen. 5 keV Ar^+ sputtering was performed for 60 s with a sample current of ~10 μA raster scanned over a 1 cm^2 area. Under such conditions, a few angstrom thick layer is removed from the surface (~5 Å for the case of polycrystalline MgO, assuming its sputtering yield for 5 keV Ar^+ to be 0.7 atoms/ion [14]). This was sufficient to remove most of the carbon. In the case of MgO, one of the O 1s and C 1s peaks were practically eliminated.

Surprisingly, after Ar^+ sputtering, the SEY *increased* for MgO but *decreased* for Al_2O_3 (Fig. 4). Two possible explanations are proposed: The first is that the carbon compound on the material has a SEY

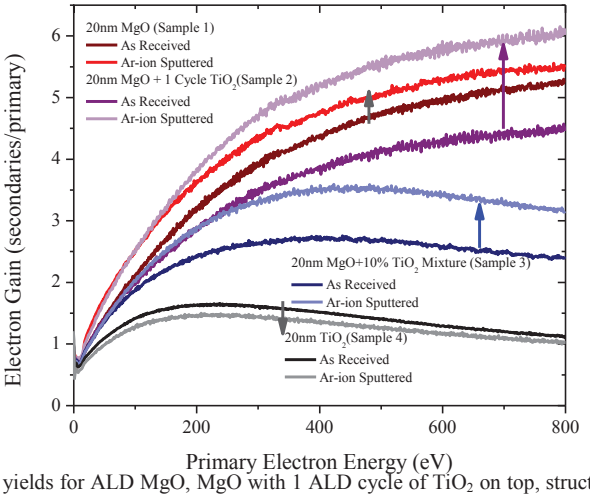

Figure 7. Secondary electron yields for ALD MgO, MgO with 1 ALD cycle of TiO_2 on top, structure consisting of alternating MgO (9 monolayers) and TiO_2 (1 monolayer) repeated to a thickness of 20 nm, and TiO_2. Also shown are the same samples after 5 keV Ar^+ sputtering. Arrows point from the as-received samples to the corresponding samples after sputtering.

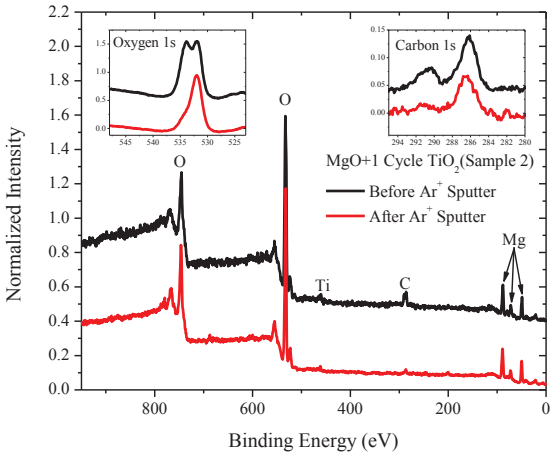

Figure 8. XPS Spectrum of ALD MgO with one cycle of TiO_2 on top (Sample 2) before and after 5keV Ar^+ sputtering. The same double carbon and oxygen peaks are visible as in Figure 5. Additionally, the Ti peak is observed at 461 eV (Figure 9). Spectra have been normalized to the O 1s peak height.

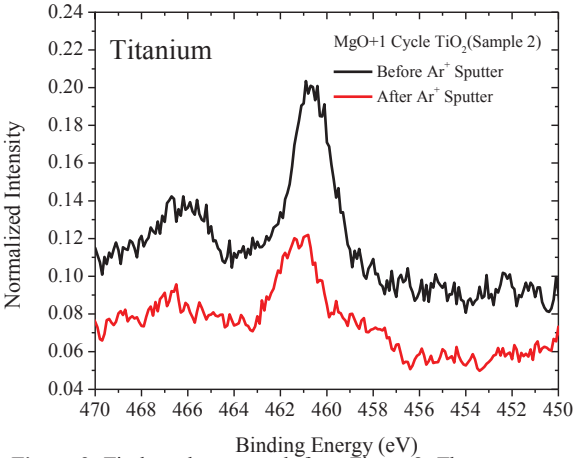

Figure 9. Ti photoelectron peak from Figure 8. The presence of this peak before and after 5 keV Ar^+ sputtering indicates that it was not entirely removed. Sputter-induced mixing of Ti into the sample may be responsible for the increase in secondary electron emission shown in Figure 7. Spectra have been normalized to the O 1s peak height.

greater than Al_2O_3 but lower than MgO. The second is supported by XPS spectra showing a different kind of bond between carbon and oxygen on the surface of the MgO sample. This bond could form a barrier for secondary electrons escaping the MgO surface. One should also recognize that Ar^+ sputtering also significantly alters the surface structure and morphology. It's likely that these changes, not observable with available equipment, affect the SEY too and thus contribute to the material's behavior described above. Moreover, at 5 keV, Ar^+ sputtering can mix surface atoms into the top layers of the sample [15] thus altering their composition and secondary electron emissive properties. Presently, it is unknown how such doping of C into Al_2O_3 or MgO would affect their secondary emission characteristics.

4.3. Layered structures (MgO/TiO_2)

A prior study showed that small amounts of TiO_2 added to MgO increased SEY from primary ions [16]. The prior report postulated that a change in band structure due to an increased presence of oxygen or an increase in stress in could be responsible for the increased SEY. While the results of Ref. [16] do not directly imply that such an increase would also be seen for primary electrons, we thought that the postulation of a change in band structure warranted an examination. It is reasonable to expect that emission of all secondary electrons, whether generated by primary electrons or ions, would be affected by this change. Characterization of surface composition and the corresponding SEY were performed on four ALD samples: MgO, MgO with the surface terminated in one monolayer of TiO_2, MgO/TiO_2 where the sample was synthesized in 9 monolayers of MgO and 1 monolayer of TiO_2 (repeating), and finally a sample of TiO_2. These samples will be referred to as Samples 1 through 4, respectively. The SEY, as generated by primary electrons, was measured before and after Ar^+ sputtering, as described in Section 4.2.

The results are summarized in Figure 7. Similar to experiments described in section 4.2, the Ar^+ sputtering caused an increase in SEY values for MgO-containing samples. In contrast, Sample 4 (pure TiO_2) showed a decrease in SEY after Ar^+ sputtering. The most noticeable change in SEY resulting from the Ar^+ sputtering was observed on Sample 2. To interpret this result, one should recognize that the ion sputtering not only removes the sample surface material, but it can also mix surface atoms into underlying layers of the material [15]. While we have no direct evidence of this ion beam mixing, the presence of Ti in the XPS spectra of Sample 2 (Figure 8) after ion sputtering suggests that some Ti was mixed within a few top-most layers of MgO (Figure 9), thus allowing it to act more as a dopant rather than an interface

Overall, the increase of the SEY caused by ion bombardment was sufficient to make Sample 2 an even more effective secondary electron emitter than the sample of pure MgO, which underwent the same ion irradiation. One may expect that a larger effect would be observed in Sample 3. However, Ar^+ sputtering was apparently brief enough that it most likely left most, if not all, of the deeper Ti monolayers untouched and intact so that the top-most layer became a doping layer while the lower layers remained to hinder the emission of secondary electrons created deeper within the sample.

5. Conclusions

These studies confirm that even minor changes in the surface composition strongly affect the secondary electron emissive properties of materials. Two proofs are presented: First, the deposition and removal by sputtering of a monolayer of TiO_2 on top of a sample of MgO (Sample 2 in the section 4.3 above). Second, carbon surface contamination from atmosphere, possibly ALD precursors, and their subsequent sputter-removal affect SEY. The XPS evidence of multiple carbon species on the surface lends support to the idea that different types of bonding between surface species and carbon might be responsible for the differences in behavior between the SEY of MgO and Al_2O_3 before and after ion sputtering. Moreover, we have to keep in consideration possible "side effects" of ion sputtering process

such as mixing and reordering of the surface. All these factors can affect the electronic band structure in the near-surface of the material and is key to defining the process of secondary electron formation.

Another key player in the SEY values is the probability of secondary electron escape from the material. The SEY vs. thickness studies show that the maximum necessary thickness for an Al_2O_3 secondary emissive coating is approximately 50 Å. In the case of MgO, sample charging hindered the investigation of materials thicker than 210 Å, and we did not reach the maximum emission even at such thicknesses. This might be connected with the differences in escape depths of secondary electrons of Al_2O_3 versus MgO (~230 Å versus ~410 Å, respectively [17]). The use of a lower electron flux may allow the measurement of thicker samples. However, this is not possible with our current setup.

For a layered TiO_2/MgO structure (a monolayer of TiO_2 on top of MgO film), we observed that Ar^+ sputtering resulted in a larger SEY increase compared to that of MgO alone. This could be a result of the incorporation of TiO_2 within the top-most layers of the sample (Ti doping due to ion beam mixing).

To conclude, this series of experiments demonstrated that for functionalization of large-area MCP surfaces, MgO is better suited than Al_2O_3 due to its increased SEY. Moreover, we demonstrated that its emissive properties can be further enhanced by adding low concentrations of other compounds such as TiO_2. This "doping" approach has a good potential and ability to finely tune properties of secondary emissive coatings, as was proven by a recent study conducted by others [18].

Acknowledgements

Work at Argonne National Laboratory was supported by the U. S. Department of Energy, Office of Science, Office of Basic Energy Sciences and Office of High Energy Physics under contract DE-AC02-06CH11357.

References

[1] LAPPD Project Website http://psec.uchicago.edu .
[2] George, S.M., Atomic Layer Deposition: An Overview, Chemical Reviews **110**, 111 (2010).
[3] Joy, D.C., UTK Metrology Group, http://web.utk.edu/~srcutk/htm/interact.htm, April 2008.
[4] Oda, O., Hanekamp, L.J., and Bootsma, G.A., App. Surf. Sci. **7**, 206 (1981).
[5] Vance, D.W., Phys. Rev. **164**, 372 (1967).
[6] Kirby, R., "Instrumental effects in secondary electron yield and energy distribution measurements" at 31st ICFA Advanced Beam Dynamics Workshop on Electron Cloud Effects, 2004.
[7] Laponsky, A.B. and Rey Whetten, N., Phys. Rev. Lett. **11**, 510 (1959).
[8] Yater, J.E. and Shih, A., J. Appl. Phys. **87**, 8103 (2000).
[9] Insepov, Z., Ivanov, V., Jokela, S., and Wetstein, M., "Comparison of Back-Scattering Properties of Electron Emission Materials" at 2011 Particle Accelerator Conference, New York, NY, USA.
[10] Lee, J., Jeong, T., Yu, S., Jin, S., Heo, J., Yi, W., Jeon, D., and Kim, J.M., Appl. Surf. Sci. **174**, 62 (2001).
[11] Meyza, X., Goeuriot, D., Guerret-Piécourt, Tréheux, D., and Fitting, H.-J., J. Appl. Phys. **94**, 5384 (2003).
[12] Ochs, D., Brause, M., Braun, B., Maus-Friedrichs, W., and Kempter, V., Surf. Sci **397**, 101 (1998).
[13] Henrist, B., Hilleret, N., Scheuerlein, C., Taborelli, M., and Vorlaufer, G., in The Proceedings of EPAC 2002, Paris, France, 2002, pp. 2553.
[14] Betz, G. and Wehner, G., Sputtering of multicomponent materials, in: R. Behrisch (Ed.), Sputtering by Particle Bombardment II. Sputtering of Alloys and Compounds, Electron and Neutron Sputtering, Surface Topography, Springer-Verlag, 1983
[15] Nawash, J.M., Masoud, N.M., Al-Saleh, K.A., and Saleh, N.S., J. Mater Sci **42**, 7488 (2007).
[16] Kim, R., Kim, Y., and Park, J.-W., Thin Solid Films **376**, 183 (2000).
[17] Rajopadhye N. R., Joglekar V. A., Bhoraskar V. N., Bhoraskar S. V., Solid State Communications **60**, 675 (1986).
[18] Yu, H.K., Kim, W.-K., Park, E.C., Kim, J.S., Koo, B.-W., Kim, Y.-W., Ryu, J.H., Lee, J.-L., J. Phys. Chem. C, Article ASAP, DOI: 10.1021/jp205759s, (2011)